Magazine of Concrete Research, 2005, **57**, No. 2, March, 101–109

The use of MRI to observe the structure of concrete

E. Marfisi*, C. J. Burgoyne*, M. H. G. Amin† and L. D. Hall†

University of Cambridge

A range of magnetic resonance imaging (MRI) measurements of water in concrete samples and their constituent materials is described and it is demonstrated that MRI can be used to (1) discriminate the spatial distribution of aggregates within a fresh sample, (2) measure changes in water content during the hardening process of cement, and (3) detect fractures and voids within a water-saturated sample. The requirements of the magnetic resonance technique that the sample be free of iron impurities necessitated an investigation of a range of materials for manufacturing suitable concrete samples. This led to a mix design which is representative of normal concretes yet MRI compatible. MRI can achieve image acquisition using a number of different protocols which are defined and optimised according to the equipment available, the properties of the sample and the particular type of image required. Suitable protocols for detecting the water in concrete are described. Magnetic resonance (MR) images of the internal structure of concrete are presented, which allow the aggregate, sand and matrix to be distinguished as well as any voids that are present. It is shown from our experiments that the measurable water present in wet concrete is in two forms, and the amount and proportions of these two components alters during hardening, which allows the progress of the associated chemical reaction to be studied. It is shown that fractures can be detected, but it is concluded that rather than attempting to determine both the structure and the fracture state from a single MRI image, it is far better to measure two separate images, one optimised to show the structure and the second for delineating the fractures.

Introduction

During the past two decades, magnetic resonance imaging (MRI) has become widely used in the medical field because it allows the visualisation of the internal structures of soft tissues in the human body by measuring their water content.[1] More recently, MRI has been applied to many other fields.[2]

The present project has been undertaken to demonstrate that MRI can be used to determine the structure and fracture state of hardened and reinforced concrete. Although it is not possible to use MRI to study concrete reinforced with steel because it distorts the MRI scans, fibre-reinforced polymer (FRP) rods are MRI compatible.[3] The work reported here has been undertaken at Cambridge as a joint project between the Cambridge University Engineering Department (CUED) and the Herchel Smith Laboratory for Medicinal Chemistry (HSLMC). This is the first of a series of three papers reporting the results of that study; it relates to determination of the internal structure of concrete and measurements of the progress of hardening. The second paper[4] shows how the fracture state of plain and reinforced concrete samples can be imaged, while the third[5] reports on tests on a reinforced concrete beam loaded inside the MR magnet to follow the progress of cracking as the load increases.

* Department of Engineering, University of Cambridge, Trumpington St, Cambridge CB2 1PZ, UK.
† Herchel Smith Laboratory for Medicinal Chemistry, University of Cambridge School of Clinical Medicine, Robinson Way, Cambridge CB2 2PZ, UK.

(MCR 41228) Paper received 5 January 2004; last revised 9 September 2004; accepted 8 October 2004

Concrete behaviour

Concrete is a conglomerate made by mixing aggregates, sand, cement and water in suitable proportions. The resulting composite material is often described by its strength and stiffness, but these are the overall and averaged properties of a notional heterogeneous material and are not sufficient to describe local variations and

their effect on the behaviour. Most experimental work on concrete is either on the micro-scale, following the growth of crystals of cement products, or on the macro-scale, where concrete is regarded as a material with strength and stiffness. Most existing techniques for determining the structure of concrete at the meso-scale are destructive since the sample has to be broken open, or drilled into, to obtain samples for analysis. This process can itself alter the structure being studied, so investigations have to be carried out numerically with only gross comparisons with experiments. Clearly, the availability of a non-invasive tool to investigate the behaviour of concrete on the meso-scale, even on laboratory-sized samples, would be a great advance.

The mechanical characteristics of concrete are widely assumed to be the result of interaction between the internal components and the influence of defects such as voids and pre-existing fractures. In reinforced concrete, the local relationship between the reinforcing bar and the concrete is the most important influence on the bond strength. Porosity, permeability, durability and fracture propagation are all aspects that require study. The properties of concrete depend on the chemistry of cement; incorrect hydration or incomplete hardening of cement paste causes defects and heterogeneity in the matrix.

The spatial distribution of all these factors and, importantly, their variation with time, are both of interest. Since the time dependencies cannot be evaluated by existing destructive methods, access to a non-invasive method for observing a concrete sample in three dimensions could answer many of the existing uncertainties and would provide a technique for direct comparison with numerical analysis. A spatial resolution of about 200 μm would allow the observation of fractures,[6,7] although study of the pores within the matrix would require a higher resolution.[6] Ultrasonic pulse velocity and dielectric constant measurements can be used to determine the degree of hydration, but they can only give indirect indications of the chemistry in the bulk specimen.

The present study was designed to evaluate the prospects for using magnetic resonance imaging (MRI) to measure some of these properties and to select the necessary MRI protocols. MRI can discriminate between different materials partly by measuring the distribution of their water content and partly by determining their MRI properties. Permeability and porosity can be determined if the changes of water content with time are measured. The observation of the internal structure is possible by making use of the high signal intensity generated by the cement paste; measurement of fractures in concrete is more difficult but possible by careful selection of the MRI parameters. The study of reinforced concrete can only be carried out if non-magnetic reinforcement is used.

It had originally been intended to design a single measurement procedure whereby it was possible to distinguish three separate components

(*a*) solid materials (e.g. aggregates)
(*b*) porous materials (e.g. the cement matrix)
(*c*) voids (either as flaws in the original structure or fractures after loading).

However, as will be explained below, that intention was modified so that two separate images are obtained, each of which can show two of the required components. The images can then be superimposed to obtain the desired result.

MR principles

MR allows the direct, non-destructive observation of both static and dynamic phenomena of fluid transport in porous media. For this reason its development has led to application in many different fields. It is appropriate in this paper only to give a brief overview of MR principles; for full details of the technique the reader is directed to the specialist literature (e.g. see Reference 1 for medical applications and Reference 2 for non-medical applications). Magnetic resonance involves the simultaneous application of a static magnetic field and radio-frequency (RF) pulses; the magnetic field aligns all the hydrogen nuclei that are present in the sample and the RF pulse changes that orientation. As the hydrogen nuclei return to their original equilibrium state, they generate a signal which is detectable by a sensitive RF receiver and is proportional to the density of hydrogen nuclei and therefore, indirectly, to the local water content. The characteristics of this returned signal allow the measurement of the bulk properties of the sample. This is known as nuclear magnetic resonance (NMR). The application of a magnetic field gradient in a defined direction gives the signal spatial discrimination, which then allows the acquisition of images. This is the MRI technique. It is possible to define a two-dimensional (2-D) slice and then to measure the spatial distribution within it. Alternatively, a complete three-dimensional (3-D) assessment can be made. The signal is also affected by the mobility of the hydrogen nuclei; although liquid water gives an MR response, its low mobility in ice prevents any signal detection. Consequently, the observation of the different internal structures inside an object depends not only on the amount of water present but also on its mobility.

Water in porous media is generally characterised by rapid decay of the magnetisation of the water protons which makes it difficult even to observe, let alone measure, its spatial distribution by MRI. In turn, this restricts the scope of MRI to measure the mobility of the water molecules and thereby to characterise the pore structure of the matrix material. Nevertheless, the water in some porous matrices does have sufficiently long relaxation times for NMR to be able to make incisive practical studies. Consequently, there is ample precedent for the use of MR to measure water content in a range of porous

media including rocks,[8–11] soils[12] and construction materials including bricks, cements and concrete.[13–16]

These papers in the literature present various applications of MR to the study of mechanical and physical phenomena in solid materials. The measurement of water content led to the study of porosity and permeability.[13] One- and two-dimensional studies followed from this work,[14] which was of particular interest because of the well-established relationship between porosity and durability in concrete.

More recently, single-point imaging (SPI) has been used to study shrinkage and drying of concrete and mortar.[17] Freeze/thaw effects have also been studied,[18] as has ion penetration.[19] However, since the image is acquired without slice selection and by points rather than line scanning, it gives poorer spatial resolution and takes much longer to acquire an image (hours rather than minutes); 3-D images have not yet been acquired by these techniques and even 2-D images can only be obtained with difficulty.

Of particular relevance are the many studies of water and/or hydrocarbon in porous rocks, which have clearly demonstrated the unique potential of MR to provide insight into the pore structures of many rocks. Importantly too, they have also identified a variety of practical problems which limit the range of materials that can be studied by MR, and in particular those associated with even small quantities of chemical compounds, such as iron and manganese ions.[20,21]

Due to the need for the sample to be in a very homogeneous magnetic field, MRI cannot be performed if there are any magnetic elements inside the sample, which precludes the use of normal steel reinforcement and some types of aggregate. The methods used to acquire the signal, the magnitude and gradient of the magnetic field applied, and their precision, can all be optimised for different samples and the time required for image acquisition is also influenced by these factors. As a consequence, the MRI technique is very flexible but the system requires calibration for each kind of investigation and knowledge of the physical characteristics of the sample is necessary to identify the factors that can influence, block or disturb the acquisition of the signal.

The MRI signal is defined by four separate parameters: the amplitude, frequency, phase and duration of the proton resonance. Two distinct NMR relaxation processes influence the amplitude and the duration of the signal from the water. The longitudinal (spin–lattice) relaxation time (T_1) is defined as the time constant of the process by which the proton magnetisation returns to its thermal equilibrium after perturbation by the RF pulse. The transverse (spin–spin) relaxation time (T_2) is the time constant for the loss of magnetisation in the transverse plane. These time constants reflect the molecular, magnetic and physical properties of the water protons in the sample, and can therefore provide insight to its material properties.

When planning a measurement, the echo time (T_E) and repetition time (T_R) that are chosen have to be optimised to reflect the actual values of T_1 and T_2 for that particular sample. T_E is the length of time for which measurement of the signal intensity is carried out, while T_R is the time that must elapse before the signal from a measurement has died away so that the next measurement can start. The time needed for signal acquisition depends on these parameters.

The values of T_1 and T_2 dictate whether or not it is possible to acquire the signal from the sample. For example, when analysing a sample of pure water with a 2-T (tesla) magnet, both of these values are around 3 s and MRI scanning is technically easy. However it is known that water in porous media material (such as rock, soil and mortar) has much lower values (by a factor of about 10–100 for T_1 and 1000–100 000 for T_2).[10–12] Inevitably this always demands higher performance from the scanner hardware, and for many samples the values may not allow sufficient signal to be generated for MRI. Although this decrease of T_1 and T_2 was expected for the water in the pore structure of intact concrete, the water present in voids or fractures should have sufficiently long T_1 and T_2 values that the use of short T_E and long T_R values would allow signal acquisition.

For structurally heterogeneous materials the signal from the sample probably comes from more than one environment and it is possible to analyse the MR signal to determine the number of components it contains, their magnitudes and their time constants.[9–11] Bulk measurements on concrete have been obtained which show three separate components.[15,16] Although this allows information to be obtained about the proportion of different components within the sample, it is difficult simultaneously to determine their spatial distribution.

In the light of the above it was appropriate to use liquid-state MRI, in which the responses from water are used to show the various structures. It must be emphasised that what is being measured in this technique is the water content; solid materials appear as low-intensity shadows against a high-intensity background from the mobile water. An alternative approach, which can investigate some solids directly, needs to acquire the signal from protons which are tightly bound. This process is much more difficult and time consuming, and gives lower resolution.[22,23]

A series of experiments were made to choose the optimal sequence for subsequent image acquisition and the spin echo sequence was selected.[1,2] This uses two RF pulses; the first alters the orientation of the spin magnetisation by 90°; the second refocusing pulse rotates this magnetic vector by 180°. The RF receiver then measures the signal generated as the proton magnetisation returns to its equilibrium state. T_R must be at least three times T_1 to ensure that the proton magnetisation has returned close to its equilibrium state before the next measurement begins. In the experiments de-

scribed here, T_E was taken as 4·5 ms to enable efficient detection of the water proton signal. T_R ranged between 100 and 1000 ms depending on the type of observation; each measurement was taken four times and the average taken to increase the signal-to-noise (S/N) level and thereby reduce the effects of background noise.

MRI equipment

The MRI scanner is based on a modified Oxford Research Systems Biospec 1 spectrometer console and a 310-mm-bore 2-T superconducting solenoid magnet (Oxford Instruments). The coils used to produce the gradient fields have a 108-mm bore and give field gradients of 1·14 Gauss/mm. The RF probe, manufactured in HSLMC, provides a cylindrical space 54 mm in diameter and 163 mm long; the field-of-view is located in the central 100 mm.

MRI spatial resolution

The MRI scanner provides spatial resolution by means of three sets of gradient coils, each of which produces a linear variation of magnetic field that induces a spatial distribution of the water proton resonance frequency in one of three orthogonal directions. The field of view was restricted to be 40×40 mm. Since the digital matrix was 256×256 pixels, the pixel resolution was 156 μm in both directions across a slice. The thickness of the slice can also be selected and it was decided to acquire 32 slices over a 40 mm length giving a slice thickness of 1250 μm. Taken together this corresponds to a 3-D sample resolution of $156 \times 156 \times 1250$ μm. Although it is possible to reduce these dimensions to increase the resolution, this reduces the amount of material producing the signal in each voxel and hence the signal-to-noise (S/N) ratio; either the time needed to image the sample has to be increased or the size of the sample reduced. The overall quality of an MRI image depends on the size of each pixel in the image plane, plus the intrinsic S/N ratio. Clearly, the smaller the pixel dimensions, the higher the spatial resolution; however, given that the S/N ratio depends on the volume defined by each pixel, the lower the S/N ratio and hence the lower the quality of the image.

A numerical procedure needs to be undertaken to determine the amount of signal that comes from each voxel. To do this, the gradient coils are used independently to adjust the signal strength in each of the three directions; in this study $256 \times 256 \times 32$ sets of readings are taken. Fast Fourier transforms are performed to determine the spatial distribution of the signal.

Material investigation

Tests were carried out on small samples of various possible materials to determine which were the most suitable components for the final concrete mix. Each was placed in a cylindrical plastic beaker (30 mm diameter by 45 mm long) filled with water. The direct observation of each material separately gave the opportunity of discriminating between their magnetic responses and also of testing the ability to acquire a signal. Two-dimensional slice MRI scans were then taken through each beaker in turn to evaluate the effect of each material on what should be a circular image—lack of circularity indicates the presence of magnetic components within the sample which distort the image.

Aggregate

Figure 1 shows images of two materials that result in distorted images. The one on the left is a sample of crushed granite which shows a strong diffuse distortion, whereas the one on the right is a sample of river gravel which shows localised distortion on the right-hand side. The magnetic components in the granite are scattered throughout the sample, whereas in the river gravel it is likely that only a few of the pieces are magnetic, while others are non-magnetic.

In contrast, Fig. 2 shows materials which are suitable for MRI. The one on the left is from a sample of limestone aggregates, where the circularity of the beaker is clearly visible and the individual pieces of stone can be identified. The image on the right shows quartz

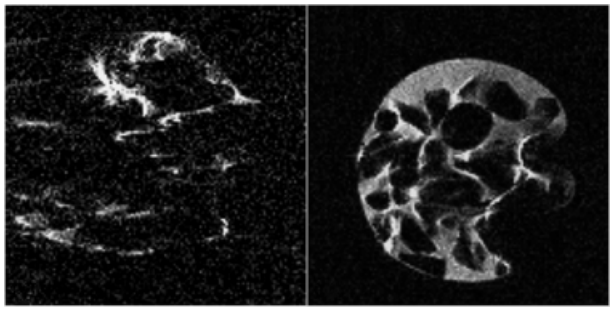

Fig. 1. Aggregates under water: (a) crushed granite; and (b) river gravel

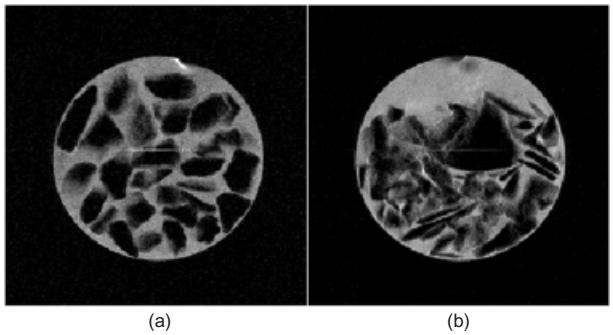

Fig. 2. Materials suitable for MRI: (a) limestone; and (b) quartz

pieces which are also clearly visible. However, because the crushed pieces had a columnar structure, they were deemed not suitable for making representative concrete. Broken glass showed similar clarity.

Figure 3 shows images from samples of silica sand, as used in the Cambridge University Engineering Department laboratory, and circular nylon balls. Both gave clear undistorted images although in the sand sample, where the amount of free water is small, the S/N ratio is quite poor. The zone outside the circular beaker was air, so the signals from that area are RF noise.

Matrix

The matrix was also studied. Various types of cement were studied by casting samples (without sand or aggregate) inside a beaker. Four rods of different sizes were cast into the cement, but removed as soon as the sample had set, to leave holes which subsequently could be filled with water to provide contrast.

A small amount of iron is a desirable component of cement; if insufficient iron is present in the calcareous or silicaceous components of the cement, iron oxide is deliberately added during manufacture. Ordinary Portland cement (OPC) is known to contain some paramagnetic materials (principally Fe_2O_3) that make up about 2–5% of the material.[24] Fig. 4(a) shows minor loss of circularity in the image of the water in the holes. White Portland cement (WPC) is manufactured for use where the colour of the concrete is important, using carefully selected clay and limestone to eliminate discolouring impurities, principally iron. No extra iron is added during manufacture. Fig. 4(b), shows that the image of a WPC sample has very little distortion from the original dimensions. However, the content of the circular beaker is not visible in either of these images which means that although both samples were saturated, the matrix has effectively suppressed the entire MRI response from the water.

In contrast, the water in plaster of Paris (gypsum), which is more porous and which should not contain any paramagnetic centres, can be detected after hardening, as is shown in Fig 4(c), where the circular holes show up as white, the plaster as grey, and the air outside the beaker as black. The white line across Fig. 4 and some of the other images is an artefact of the test set-up used.

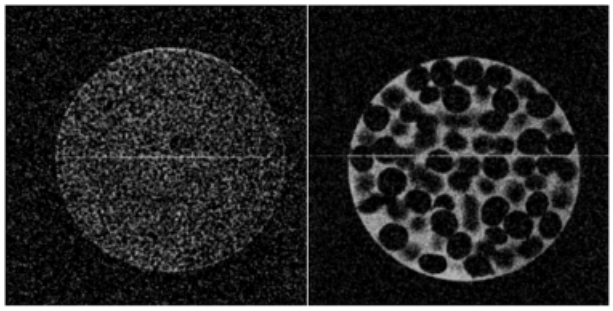

Fig. 3. MRI image from samples of: (a) silica sand; and (b) nylon balls

Concrete

Figure 5 shows three samples of hardened concrete. It follows from the above that a combination of aggregates and cement (OPC or WPC) should suppress the observation of the internal structure of a hardened concrete sample and the sample on the left, with WPC and limestone, shows virtually no internal structure. However, the images in the centre and on the right both show the structure clearly. They were both made by mixing cement and plaster in different proportions, with that on the right from a sample with a 50/50 plaster/WPC mix. This suggested the possible use of such mixtures as the basis for the remainder of this study. However, the presence of plaster significantly alters the failure mechanism of the resultant concrete, which has a much more plastic behaviour and a very different fracture mechanism. Compression tests on different plaster/cement mixes showed that only samples with a very small amount of plaster gave a fracture behaviour that was representative of normal concrete;

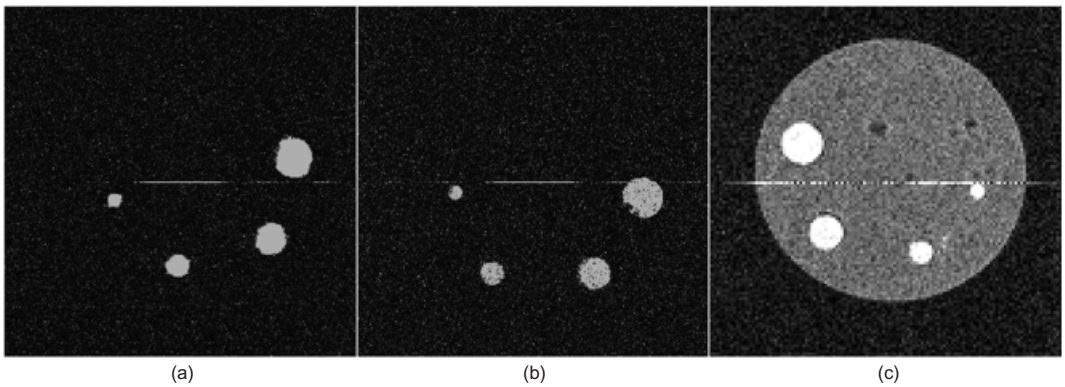

Fig. 4. Matrix with holes full of water: (a) OPC; (b) WPC; and (c) plaster

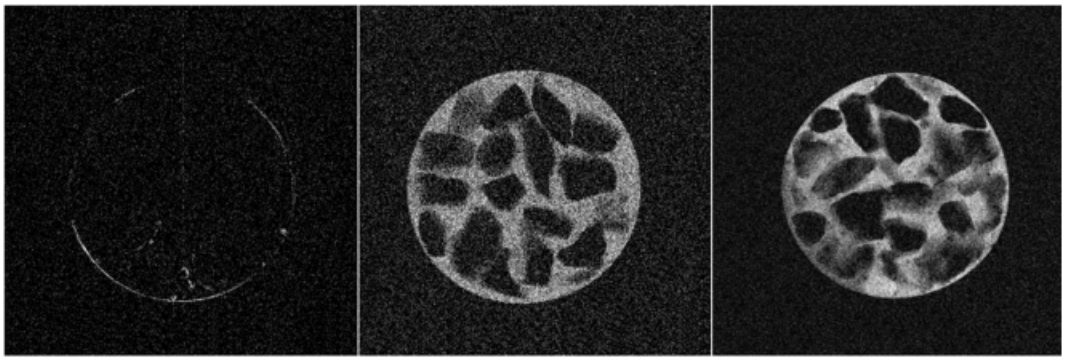

Fig. 5. Effect of WPC/plaster ratio on visibility of structure in hardened concrete: (a) WPC and limestone; (b) plaster and limestone; and (c) WPC, plaster and limestone

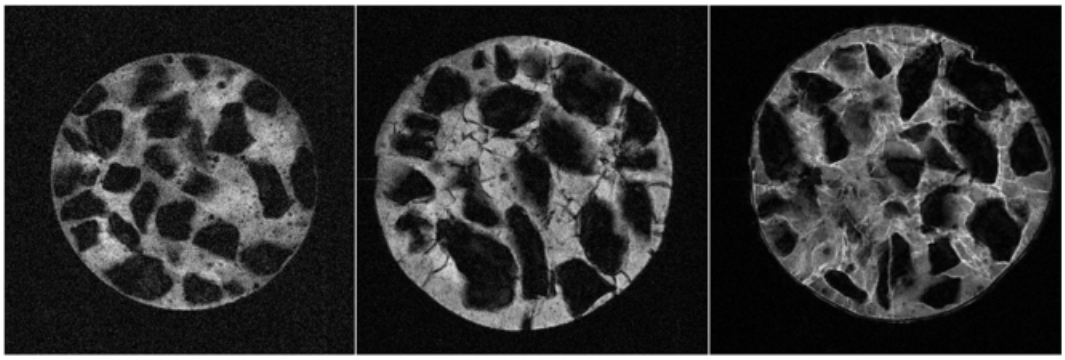

Fig. 6. Hardened saturated sample with 50% plaster mix: (a) structure; (b) air in fractures; and (c) water in fractures

unfortunately none of these showed detailed internal structure in their MRI scans.

Studies of samples made from 50% plaster and 50% WPC provided useful insight into the effect of fractures on the MRI images. Fig. 6(a) shows the hardened but uncracked sample in which the aggregate, matrix and air outside the beaker are clearly distinguishable. The same sample was then loaded in compression to produce fractures which filled with air as shown in Fig. 6(b). The fractures are just visible as dark lines against the background, but are not easy to detect. The sample was then placed in a vacuum to remove the air, and allowed to fill with water, which penetrated at least the large cracks which were connected to the outside of the sample, but may not have penetrated into isolated internal flaws. Fig. 6(c) shows this image, where the fractures are clearly visible as white lines. No attempt was made to align the three images shown in Fig. 6, so although they relate to the same sample they do not show the same slice and the fractures and structure differ in the three images.

These three images demonstrate the problems associated with trying to obtain information about structure and fracture from the same image. Even with a porous matrix material, like the 50/50 plaster/WPC mix, the matrix does not appear uniformly grey. The fractures, which are of similar or smaller dimensions to the pixel resolution, do not appear to be completely black (if filled with air in Fig. 6(b)) or completely white (if filled with water in Fig. 6(c)). It is thus very difficult to determine, by looking at a grey pixel, how much of the 'greyness' comes from the matrix, and how much from the crack. Although, at first sight, Fig 6(c) appears to contain all the information that is being sought, it is impossible to extract information from it in a more useful way.

As a result of this observation, it was decided not to pursue the original idea of obtaining aggregate, matrix and fracture distributions from a single image, nor to pursue the use of plaster as a cementing material. Instead, it was decided to use WPC as the cement; the solid hardened sample would scan as a purely black image and any whiteness in the image of a water-saturated sample would have to be due to the presence of fractures or pre-existing voids in the structure. Important information about the fracture pattern can be determined, and this process will be discussed in a later paper.[4] An image of the structure can be obtained soon after casting as there is a significant amount of free water in the sample.

A corollary of that decision is that some form of image registration would be required so that a sample

could be scanned on two (or more) separate occasions and the resulting images aligned so that the relationship between structure and fracture could be determined.

Hardening of cement paste

Once it had been decided to obtain the structure image soon after casting, it was sensible to investigate the hardening process to determine the timescale over which the structure could be determined. The MR signal from the protons of water depends on the overall mobility of the water molecules, which is a function of their interaction with different chemical compounds in the surrounding matrix. The hardening process transforms the water and cement powder into a solid material and this gradually decreases the MRI signal of the sample to zero. Hydrogen nuclei present in hydrates and hydroxides are physically much more tightly bound than those in free water and hence, during curing of concrete, their T_1 and T_2 values decrease significantly. As a result, the efficiency with which the original water content is detected by MRI progressively decreases as the concrete cures, and is eventually undetectable. Consequently, the hardening process can be followed by measuring the progressive loss of MRI intensity.

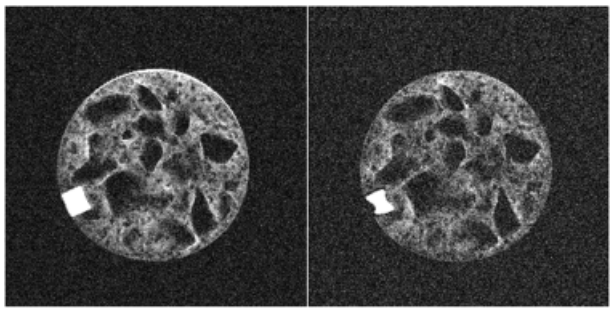

Fig. 7. The effect of hardening: (a) 1 h after casting; and (b) 8 h after casting

The presence of free water immediately after casting allows the generation of a strong MRI signal from the fresh cement paste which can be used to determine the heterogeneity of the cement paste by identifying local differences in water content or unhydrated regions. It also allows the aggregate to be distinguished from the matrix. Fig. 7 shows two scans of the same WPC/limestone/sand concrete sample. The first was taken one hour after casting and the aggregate and sand samples can clearly be seen. The white square on the left-hand side is a piece of potato that was placed on the side of the plastic beaker in which the sample was cast. The potato is stiff enough to retain its shape when the concrete was cast but, as it is virtually full of water, shows up very clearly in the image. The second image of the same slice, taken 7 h later, shows the details of the matrix less clearly as the cement paste has hardened, although the strongly hydrophilic cement has sucked water from the potato, distorting it. The square void formed by the potato is still clearly visible; as is demonstrated in the second paper,[4] this void could be filled with water for added clarity.

It is also possible to measure the T_1 and T_2 values of the protons of the water in the bulk sample at different times during the hardening process. If the sample contains water with different mobilities, the measured signal from their protons can contain multiple components, and it is possible to recover the T_1 and T_2 values from each component separately.[11]

These effects are illustrated by a series of measurements that were carried out on a sample made from limestone aggregate and WPC cement over the four weeks following casting. The sample was cured under water and its surface was dried before each measurement to eliminate the MR signal from free water on the

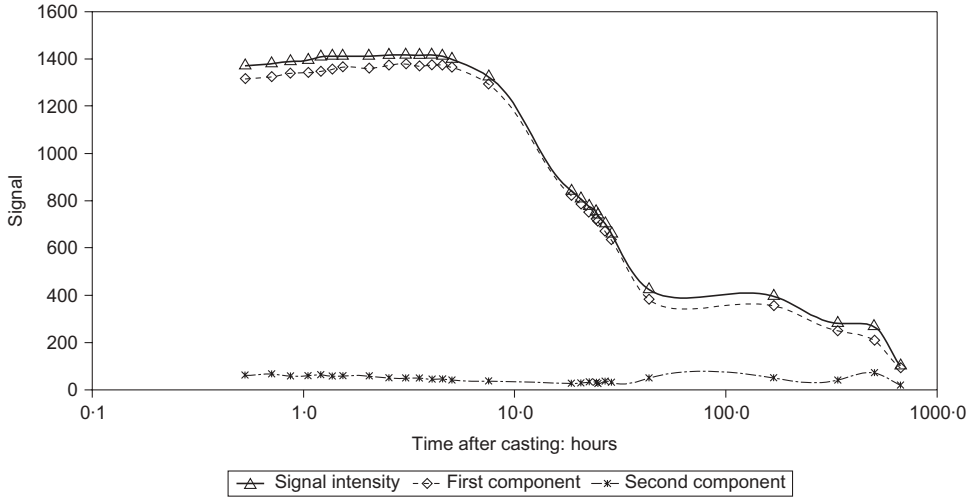

Fig. 8. Variation of signal intensity of the two water components in the matrix, as determined from the T_2 measurements

surface of the sample, which would swamp that from the water in the concrete itself.

It was observed that the matrix gave a signal from two separate components with T_E of 0·8 ms in a 2-T magnet. Straight after casting, 98% of the signal came from the first component. The variation with time of the signal intensity reconstructed using T_2 values from these two components is shown in Fig. 8 for a period of 28 days (672 h). This time was chosen because modern cements are designed so that their hardening reactions are then virtually complete. The water in concrete can be in three forms[15]

(*a*) free water in the pores between the cement grains
(*b*) water which is chemically unchanged but is physically bound to the surface of the cement or aggregate
(*c*) water in the form of hydrates and hydroxides in the products of the chemical reaction.

The last component is expected to give a very weak signal since the hydrogen atoms (i.e. protons) are very tightly constrained and hence their MR signal will decay so rapidly that it cannot be detected. Hence it is believed that the first MR signal component represents the free water, while the second component represents the bound water.

No significant changes of signal were measured during the first 4 h, and even at 10 h the contrast is still sufficiently clear to distinguish the aggregate from the background. This implies that the rapid setting reaction of the cement paste, which takes place in the first 2 or 3 h, does not significantly alter the MRI signal, in contrast to the subsequent hardening reaction. Hence during the first 10 h it would be possible to distinguish the aggregate from the matrix, even in concrete made from WPC.

Although the two components are clearly different at the beginning of curing it becomes more difficult to distinguish them as time goes on. This phenomenon is linked to the reduction in mobility of water as hardening takes place. Between 8 and 50 h after casting there is a large reduction in the first T_2 component and the signal continues to decrease as the hardening reaction moves to completion while the free water reacts with the cement. Once hardening has been completed the MRI signal intensity is so low that it is very difficult to determine internal structure within the hardened concrete.

Study of fracture

The second paper in this series extends this use of MRI to the visualisation of fractures within concrete samples, and demonstrates that it is possible to combine images of fractures with those of structure to study the relationship between fractures and the internal structure of concrete.

Conclusion

It has been shown that MRI techniques can be used to investigate the behaviour of concrete on the mesoscale. MRI imaging detects the presence of water and is most sensitive to free water that is not bound either physically or chemically. It has been necessary to use materials in the concrete that do not interfere with the magnetic fields used in the scanner; granite and some river gravels are shown to be unsuitable, but white limestone and quartz are suitable, as are silica sands.

Liquid-state MRI, using a spin echo protocol with an echo time of 4·5 ms, and a repetition time of 100 ms has been found to be suitable. For a 2-D slice 1·25 mm thick, a spatial resolution of 156×156 μm has been obtained, using a 256×256 digital matrix. Four measurements have to be taken of each signal and averaged and the total scan time is 1·7 min. Alternatively, a 3-D image set $156 \times 156 \times 1250$ μm requires 55 min of scanning time.

Although OPC contains only a small amount of iron, it is unsuitable as a cementing material for MRI studies, whereas WPC has been shown to give clear images. It is possible to see the structure of concrete for a few hours after casting, but as the water becomes bound to the cement surface or reacted to form hydroxides, it becomes almost invisible. Plaster of Paris has also been shown to give clear images and as it is slightly porous it allows the structure to be observed even after hardening. This visibility persists when a small proportion of plaster is mixed with WPC, but the plaster significantly alters the fracture process in the resultant concrete which is not representative of structural concrete.

It has been shown that it is possible to measure the response from two separate components during the hardening process. The proportions of these components change with time, which allows the progress of the reaction to be observed, and would allow the effects of differential hardening across a sample to be studied.

Finally, it has been concluded that it is not feasible to obtain a single image that distinguishes aggregate, matrix and fractures. This is partly because the MRI visibility of the structure decreases as hardening takes place, and partly because when both matrix and fractures are present in the same image it is difficult to distinguish between them, as they both show up as different levels of grey. Thus it is preferable to take one image which clearly shows the structure, and subsequently a second image to show the fractures in high contrast from the solid components.

This is the key strategic innovation of this study since it enables MRI to be used to study both the internal geometry of a concrete sample to locate internal defects and also to measure fractures subsequently induced. MRI can also be used to study the hardening of concrete samples and by observing the water content, allows the study of the chemistry of cement and concrete. Hence it is now clear that MRI is a powerful,

non-invasive tool for the study of the meso-structure of concrete.

Acknowledgments

This work was supported by the EU TMR Network 'ConFibreCrete' and by the Herchel Smith Endowments.

References

1. Mansfield P. and Morris P. G. *NMR Imaging in Biomedicine*. Academic Press, London, 1982.
2. Callaghan P. T. *Principle of Nuclear Magnetic Resonance Microscopy.* Clarendon Press, Oxford, 1991.
3. Nanni A. (ed.) *Fibre Reinforcing for Concrete Structures: Properties and Applications*. Elsevier, Amsterdam, 1993.
4. Marfisi E., Burgoyne C. J., Amin M. H. G. and Hall L. D. The use of MRI to observe fractures in concrete. *Magazine of Concrete Research*, 2005, **57**, No. 2, 113–123.
5. Marfisi E., Burgoyne C. J., Amin M. H. G. and Hall L. D. Observation of flexural cracks in loaded concrete beams using MRI, *Magazine of Concrete Research*, 2005, **57**, (in press).
6. van Mier J. G. M. *Fracture Processes of Concrete—Assessment of Material Parameters for Fracture Models*. CRC Press, Boca Raton, Florida, USA, 1997.
7. Wittmann F. H. Fracture mechanics of concrete. *Developments in Civil Engineering*, Elsevier, Amsterdam, 1983.
8. Gummerson R. J., Hall C., Hoff W. D., Hawkes R., Holland G. N. and Moore W. S. Unsaturated water flow within porous materials observed by NMR imaging. *Nature*, 1979, **281**, 56–57.
9. Carpenter T. A., Davies E. S., Hall C., Hall L. D., Hoff W. D. and Wilson M. A. Capillary water migration in rock: process and material properties examined by NMR imaging. *Materials and Structures*, 1993, **26**, No. 159, 268–292.
10. Kleinberg R. L., Straley C., Kenyon W. E., Akkurt R. and Farooqui S. A. Nuclear magnetic resonance of rocks: T_1 vs T_2. *SPE International,* 1993, Society of Petroleum Engineers paper 26470.
11. Kleinberg, R. L., Kenyon W. E. and Mitra P. P. Mechanism of NMR relaxation of fluids in rock. *Journal of Magnetic Resonance A*, 1994, **108**, No. 2, 206–214.
12. Hall, L. D., Amin M. H. G., Dougherty E., Šanda M., Votrubová J., Richards K.S., Chorley R.J. and Císlerová M. MR properties of water in saturated soils and resulting loss of MRI signal in water content detection at 2 tesla. *Geoderma*, 1997, **80**, No. 3/4, 431–448.
13. Kaufmann J., Stunder W., Link J. and Schenker K. Study of water suction of concrete with magnetic resonance imaging methods. *Magazine of Concrete Research*, 1997, **49**, No. 180, 157–165.
14. Valckenborg R. M. E., Pel L., Hazrati K., Kopinga K. and Marchand J. Pore water distribution in mortar during drying as determined by NMR. *Materials and Structures*, 2001, **34**, No. 224, 599–604.
15. Best G., Cross A., Peemoeller H. and Pintar M. M. Distribution of pore sizes in white concrete. *Proceedings of the Materials Research Society Symposium*, 1995, **370**, 271–277.
16. Dobmann G., Kroenig M., Surkowa N., von Bernus L. and Wolter B. The potential of nuclear magnetic resonance (NMR) to non-destructively characterize early-age concrete by a one-sided access (OSA) technique. *Proceedings of the Non Destructive Evaluation 2002 Seminar,* Chennai, 2002, paper 091.
17. Beyea S. D., Balcom B. J., Bremner T. W., Prado P. J., Cross A. R., Armstrong R. L. and Grattan-Bellew P. E. The influence of shrinkage-cracking on the drying behaviour of white Portland cement using single-point imaging (SPI). *Solid State Nuclear Magnetic Resonance*, 1998, **13**, No. 1–2, 93–100.
18. Prado P. J., Balcom B. J., Beyea S. D., Bremner T. W., Armstrong R. L. and Grattan-Bellew P. E. Concrete freeze/thaw as studied by magnetic resonance imaging. *Cement and Concrete Research*, 1998, **28**, No. 2, 261–270.
19. Cano F. de J., Bremner T. W., McGregor R. P. and Balcom B. J. Magnetic resonance imaging of H, Na and Cl penetration in Portland cement mortar. *Cement and Concrete Research*, 2002, **32**, No. 7, 1067–1070.
20. Tollner, E. W., Verma B. P., Malko J. A., Syhuman L. M., and Cheshire J. M. Effect of soil total iron on magnetic resonance image quality. *Communications in Soil Science and Plant Analysis*, 1991, **22**, No. 19/20, 1941–1948.
21. Foley I., Farooqui S. A. and Kleinberg R. L. Effect of paramagnetic ions on NMR relaxation of fluids at solid surfaces. *Journal of Magnetic Resonance A*, 1996, **123**, No. 1, 95–104.
22. Jezzard P., Attard J. J., Carpenter T. A. and Hall L. D. Nuclear magnetic resonance imaging in the solid state. *Progress in NMR Spectroscopy*, 1991, **23**, 1–41.
23. Szolmolanyi P., Goodyear D., Balcom B. and Matheson D. Spiral-Sprite: A rapid single point MRI technique for application to porous media. *Magnetic Resonance Imaging*, 2001, **19**, No. 3–4, 423–428.
24. Wilby G. B. *Structural Concrete—Materials; Mix Design; Plain, Reinforced and Prestressed Concrete: Design Tables*. Butterworth, London, 1983.

Discussion contributions on this paper should reach the editor by 1 September 2005